Original Article

MOLECULAR METABOLISM

Estrogen receptor-α in female skeletal muscle is not required for regulation of muscle insulin sensitivity and mitochondrial regulation

Melissa R. Iñigo [1], Adam J. Amorese [1], Michael D. Tarpey [1], Nicholas P. Balestrieri [2], Keith G. Jones [2], Daniel J. Patteson [2], Kathryn C. Jackson [6], Maria.J. Torres [3], Chien-Te Lin [2], Cody D. Smith [1], Timothy D. Heden [3], Shawna L. McMillin [3], Luke A. Weyrauch [3], Erin C. Stanley [3], Cameron A. Schmidt [1], Brita B. Kilburg-Basnyat [5], Sky W. Reece [5], Christine E. Psaltis [5], Leslie A. Leinwand [8], Katsu Funai [1,2,3], Joseph M. McClung [1,2], Kymberly M. Gowdy [2,5], Carol A. Witczak [1,2,3,4], Dawn A. Lowe [7], P. Darrell Neufer [1,2,3], Espen E. Spangenburg [1,2,3,*]

ABSTRACT

Objective: Estrogen receptor-α (ERα) is a nuclear receptor family member thought to substantially contribute to the metabolic regulation of skeletal muscle. However, previous mouse models utilized to assess the necessity of ERα signaling in skeletal muscle were confounded by altered developmental programming and/or influenced by secondary effects, making it difficult to assign a causal role for ERα. The objective of this study was to determine the role of skeletal muscle ERα in regulating metabolism in the absence of confounding factors of development.
Methods: A novel mouse model was developed allowing for induced deletion of ERα in adult female skeletal muscle (ERαKO^{ism}). ERαshRNA was also used to knockdown ERα (ERαKD) in human myotubes cultured from primary human skeletal muscle cells isolated from muscle biopsies from healthy and obese insulin-resistant women.
Results: Twelve weeks of HFD exposure had no differential effects on body composition, VO_2, VCO_2, RER, energy expenditure, and activity counts across genotypes. Although ERαKO^{ism} mice exhibited greater glucose intolerance than wild-type (WT) mice after chronic HFD, *ex vivo* skeletal muscle glucose uptake was not impaired in the ERαKO^{ism} mice. Expression of pro-inflammatory genes was altered in the skeletal muscle of the ERαKO^{ism}, but the concentrations of these inflammatory markers in the systemic circulation were either lower or remained similar to the WT mice. Finally, skeletal muscle mitochondrial respiratory capacity, oxidative phosphorylation efficiency, and H_2O_2 emission potential was not affected in the ERαKO^{ism} mice. ERαKD in human skeletal muscle cells neither altered differentiation capacity nor caused severe deficits in mitochondrial respiratory capacity.
Conclusions: Collectively, these results suggest that ERα function is superfluous in protecting against HFD-induced skeletal muscle metabolic derangements after postnatal development is complete.

Keywords Estrogen receptor-alpha; Skeletal muscle; Metabolism; Insulin sensitivity; Inflammation; Mitochondrial function

1. INTRODUCTION

Reductions in estrogen action are associated with an increased risk of developing obesity, peripheral insulin resistance, and overt Type 2 Diabetes [1–4]. Conversely, in certain situations, administering supraphysiological levels of estrogen decreases adiposity and improves peripheral insulin sensitivity [5–7]. Observational studies in the 1970s documented that the use of conjugated equine estrogen (CEE) increases the risk of endometrial cancer [8]. The largest randomized control trial study on postmenopausal hormone therapy, the Women's Health Initiative (WHI), found statistical associations between estrogen therapies and increased incidence of breast cancer, coronary heart disease, stroke, and pulmonary embolism [9,10]. Recent re-analyses of the WHI data revealed that estrogen therapies do not increase the risk of adverse events in healthy women who are within 10 years of menopause and less than 60 years of age, but the risk remains high in 70- to 79-year-old women [11,12]. The Position Statement of the North American Menopause Society in 2017 emphasized that estrogen

[1]East Carolina University Brody School of Medicine, Department of Physiology, Greenville, NC, USA [2]East Carolina University, East Carolina Diabetes and Obesity Institute, Greenville, NC, USA [3]East Carolina University, Department of Kinesiology, Greenville, NC, USA [4]East Carolina University, Department of Biochemistry and Molecular Biology, Greenville, NC, USA [5]East Carolina University Brody School of Medicine, Department of Pharmacology and Toxicology, Greenville, NC, USA [6]University of Maryland, School of Public Health, Department of Kinesiology, College Park, MD, USA [7]University of Minnesota, Department of Rehabilitation Medicine, Division of Rehabilitation Science and Division of Physical Therapy, Minneapolis, MN, USA [8]University of Colorado, Department of Molecular, Cellular, and Developmental Biology and BioFrontiers Institute, Boulder, CO, USA

*Corresponding author. East Carolina University Brody School of Medicine, 115 Heart Drive, ECHI Mail Stop 743, East Carolina University, Greenville, NC, 27834, USA. E-mail: spangenburge14@ecu.edu (E.E. Spangenburg).

Received October 14, 2019 • Revision received December 16, 2019 • Accepted December 17, 2019 • Available online 23 December 2019

https://doi.org/10.1016/j.molmet.2019.12.010

therapy prescriptions must be individualized to minimize the risks [11]; thus, understanding estrogen-mediated mechanisms across all tissues is critical.

Estrogen action on individual tissues is predominantly mediated by cell type expression of estrogen receptors (ERs) [13] and estrogens' affinity for each of the expressed receptors [14]. Previous studies suggested that ERs have numerous functions across a variety of tissues [15,16], with genomic signaling being the dominant form of regulation. The two ERs in mammals, ERα and ERβ, regulate the expression of target genes by binding to defined consensus estrogen response elements (EREs, 5′-GGTCAnnnTGACC-3′) that are generally but not always located in the 5' regulatory region of the gene [17]. Estrogens bind to the ligand-binding domain of ERs resulting in the translocation of estrogen-ER complexes to the nucleus and subsequent binding to the EREs, thus modulating gene expression [17,18].

ERα appears to play the most prominent role in skeletal muscle and potentially the regulation of glucose and lipid homeostasis [19,20]. ERα is the most abundant ER expressed in skeletal muscle [19,21]. Male and female global ERα knockout mice (ERαKO) exhibit excess visceral adiposity and skeletal muscle insulin resistance [19,22–24], whereas global ERβKO mice have normal body mass, fat mass, and insulin sensitivity [23,24]. Tissue-specific ERα loss-of-function models have led to the dissection of regulatory functions of ERα in various organs. For example, induced knockdown of liver ERα by injection of adeno-associated virus-Cre in 2-3-month-old male ERα-floxed mice results in hepatic steatosis with a modest increase in fasting glucose that is attributed to decreased inhibition of gluconeogenic enzymes in the liver [25]. Surprisingly, conventional liver-specific ERαKO mice, which develop with no liver ERα function, are similar to wild-type controls in body mass, fat mass, and glucose tolerance, even after a 5-month high-fat diet (HFD) [26]. The disparity between these findings from 2 different loss-of-function approaches emphasize the importance of conducting studies on ERα function without the confounding factors of development.

To date, only one study has investigated the role of skeletal muscle-specific ablation of ERα in the regulation of glucose and lipid homeostasis. Skeletal muscle-specific ERα function was ablated using MCK-Cre (MERKO mice), which theoretically induces deletion of ERα as early as day 13 post–conception [20,27]. Female MERKO mice exhibited increased visceral adiposity and reduced insulin sensitivity at 7 months of age [20], which was associated with the significant accumulation of lipid intermediates [20] similar to the metabolic phenotype of global ERαKO mice [19]. In C2C12 myotubes, ERα knockdown by lentiviral-ERαshRNA drastically lowered basal and ADP-supported maximal O_2 consumption, ATP production, and fatty acid oxidation rates by approximately 40–50% [20]. These findings suggest that skeletal muscle-specific ERα may be critical for preventing significant increases in adiposity as well as maintaining insulin sensitivity and mitochondrial function in adult mice. However, due to the deletion of ERα during the developmental programming stages of the skeletal muscle, this potential confounding factor could have significantly affected the interpretation of the results.

In the present study, we generated a novel inducible skeletal muscle-specific ERα knockout (ERαKO^{ism}) mouse model. We removed ERα function in mice at 10–12 weeks of age. The purpose of this study was to determine whether skeletal muscle-specific ERα is necessary to maintain metabolic homeostasis in adult female mice under lipid overload conditions. We hypothesized that the loss of skeletal muscle-specific ERα would increase the susceptibility to develop HFD-induced metabolic dysfunction. Surprisingly, this study's major finding was that ablation of skeletal muscle ERα in adult female mice did not substantially affect the response to HFD, suggesting that estrogens' protective effect in the skeletal muscle of adult mice is not mediated by ERα.

2. MATERIALS AND METHODS

2.1. Study design

2.1.1. Animal study

To assess the *in vivo* role of ERα, specifically in skeletal muscle, we generated a tamoxifen-inducible skeletal muscle-specific ERα knockout (ERαKO^{ism}) mouse model. The objective of this study was to determine the role of skeletal muscle-specific ERα in regulating metabolic function in the absence of confounding factors of development. In this model, loss of function of ERα only occurs after adult mice (10–12 weeks of age) are injected with tamoxifen, which activates Cre recombinase and induces the recombination of flox sites on exon 3 of ESR1 (ERα gene). The mice were divided into 4 groups based on genotype and diet: wild-type (WT) and ERαKO^{ism} on a control (low-fat) diet (CD) or high-fat diet (HFD). All mice were given water and food ad libitum in a room on a 12 h light/dark cycle. Ten weeks after injection, the mice underwent a transition to individual housing and a low-fat/control diet (CD) (2 days on a mixed standard chow and low-fat/control diet). After all mice were transitioned to the CD, the mice assigned to the HFD group were then fed the HFD for 12 weeks while those assigned to the CD group remained on the CD. The CD (Research Diets) contained 10% fat, 70% carbohydrates, and 20% protein while the HFD contained 45% fat, 35% carbohydrates, and 20% protein (Research Diets). Both diets had no detectable phytoestrogens. Whole body and skeletal muscle metabolic function were assessed after acute (1 week) and chronic (12 weeks) exposure to the CD or HFD. In all experiments, the mice were anesthetized with vaporized isoflurane. All of the experiments were approved by the Institutional Review Committee of East Carolina University.

2.1.2. Human cell study

This study also examined the role of skeletal muscle ERα in regulating mitochondrial respiration in human myotubes using an adenovirus-shRNA driven approach. Comparisons were made between myotubes that were cultured from primary human skeletal muscle cells isolated from muscle biopsies of healthy and obese insulin-resistant (OIR) young adult women. East Carolina University's institutional review board approved all experiments.

2.2. Ablating estrogen receptor-α (ERα) function in skeletal muscle

2.2.1. Generation of inducible skeletal muscle-specific ERα knockout mice

ERα$^{flox/flox}$ mice, which carry ESR1 with exon 3 flanked by loxP sites (provided by Dr. K. Korach, National Institute of Environmental Health Sciences), were crossed with a tamoxifen-inducible Cre (mER-Cre-mER) transgenic line driven by human α-skeletal actin promoter (HSA-MCM) (provided by Drs. K. Esser and J. J. McCarthy, University of Kentucky College of Medicine). To determine whether the offspring possessed ERα$^{flox/flox}$ and HSA-MCM, the mice were genotyped via polymerase chain reaction (PCR) using the following primer sets: 1) ERα$^{flox/flox}$ F: 5′-GACTCGCTACTGTGCCGTGTGC-3′ and R: 5′-CTTCCCTGGCATTACCACTTCTCCT-3′ and 2) HSA-MCM F: 5′-GGCATGGTGGAGATCTTTGA-3′ and R: 5′-CGACCGGCAAACGGACA-GAAGC-3′.

In this model, Cre recombinase is activated only when tamoxifen binds to mutated estrogen receptor (mER) and is not activated by endogenous estrogens [28]. Adult female mice (10–12 weeks of age) with $ER\alpha^{flox/flox}$ x HSA-MCM were intraperitoneally injected with 2 mg of tamoxifen (Millipore Sigma) once a day for 5 days as previously described [29] to induce the recombination of flox sites on exon 3. In parallel, their $ER\alpha^{flox/flox}$ x HSA-MCM littermates were injected with vehicle and served as the control (WT) mice. The mice were further aged for 10 weeks before any experiments and diet treatments were performed to ensure the washout of tamoxifen and that ERα protein was no longer detected in their skeletal muscle. The successful recombination of ESR1 and loss of ERα mRNA and protein were confirmed using PCR, RT-qPCR, and immunoblotting, respectively (Supplementary Figure S1). DNA was extracted using a Puregene Tissue Kit (Qiagen). PCR was performed using a HotStarTaq Plus Master Mix Kit (Qiagen) with the following primers: primer 1, 5′-TTGCCCGATAACAATAACAT-3′ and primer 2, 5′ GGCATTAC-CACTTCTCCTGGGAGTCT-3′.

2.2.2. Silencing ERα in human myotubes

Primary human skeletal muscle cells (HSKMCs) were provided by Dr. K. Funai (East Carolina University, Department of Kinesiology). HSKMCs were isolated from vastus lateralis muscle biopsies of healthy and obese insulin-resistant adult women. The HSKMCs were differentiated into myotubes using standard methods. Briefly, the HSKMCs were grown in DMEM with 5 mM glucose (Gibco) supplemented with 10% fetal bovine serum, Lonza SkGM SingleQuot (Lonza) without gentamicin and insulin, and 100 mg/mL penicillin-streptomycin (Gibco). At 90% confluency, differentiation was induced using DMEM with 5 mM glucose (Gibco) supplemented with 2% heat-inactivated horse serum (Gibco), 0.3% bovine serum albumin (Millipore Sigma), 0.05% fetuin (Millipore Sigma), and 100 mg/mL penicillin-streptomycin (Gibco). On the first day of differentiation, human myotubes were transduced with either scrambled shRNA (Ad-U6-shRNA-RFP) or RFP-tagged ESR1-shRNA adenovirus (Ad-RFP-U6-h-ESR1-shRNA) that targets the coding region of ERα, both purchased from Vector Biolabs. Polybrene (SCBT) was used to increase the transduction efficiency. Adenovirus infection was confirmed by imaging myotubes using a fluorescence microscope (EVOS FL Auto Cell Imaging System). No differences in the differentiation potential were observed (data not shown). Cells at passage 4–5 were used in all the experiments.

2.3. Experimental procedures

2.3.1. Body composition and food intake

Body mass and food intake were recorded weekly, and data from baseline (at 20–22 weeks of age/10 weeks post-tamoxifen or vehicle injection) until the 11th week of HFD treatment were analyzed. Fat mass and lean mass were measured using an EchoMRI-500 Body Composition Analyzer (EchoMRI, Houston, TX, USA) according to the manufacturer's protocol.

2.3.2. Indirect gas calorimetry

O_2 consumption (VO_2), CO_2 production (VCO_2), energy expenditure (H), and spontaneous cage activity levels of the mice were measured using a TSE LabMaster System (TSE Systems, Chesterfield, MO, USA) according to the manufacturer's protocol. Calorimetry data were normalized to lean body mass. Activity levels were based on the absolute number of times infrared sensors in the x, y, and z planes were disturbed. All the data were presented as the average of at least two 12-h light and dark cycles. Measurements were conducted at baseline, during the acute switch from the CD to HFD (first 2–3 days on HFD), and at the eleventh week of diet treatment.

2.3.3. Fasting insulin and glucose

The mice were fasted for 12 h. Serum insulin was measured using a commercially available kit (Millipore Sigma). A glucometer was used to measure glucose from blood drawn at the tail vein.

2.3.4. Glucose and insulin tolerance tests

Glucose tolerance was measured at the end of the 1st week and the 11th week of diet treatment. The mice were fasted for 12 h. A glucose bolus of 2 mg/kg of body mass was injected in the intraperitoneal (IP) region. Insulin tolerance was measured on a separate set of 12-h fasted mice at the end of the 11th week of diet treatment. The mice were IP injected with 0.5U insulin (Humulin, Eli Lilly). A glucometer was used to measure glucose from blood drawn at the tail vein. The mice were sacrificed 1 week after the last tolerance test (after chronic HFD) was performed.

2.3.5. *Ex vivo* skeletal muscle glucose uptake

Extensor digitorum longus and soleus muscles were dissected from the 12-h-fasted mice and used to measure glucose uptake as previously described [30]. Briefly, the muscles were incubated in 37 °C gassed (95% O_2, 5% CO_2) Krebs Ringer Bicarbonate (KRB) buffer supplemented with 2 mM pyruvate for 60 min and stimulated in the absence or presence of insulin (600 μU/mL) for 20 min. The muscles were transferred to vials containing 30 °C KRB buffer supplemented with 1.5 μCi/ml [^{3}H]-2-deoxyglucose, 1 mM 2-deoxyglucose, 0.45 μCi/ml [^{14}C]-mannitol, and 7 mM mannitol with and without insulin for 10 min and frozen in liquid nitrogen. The muscles were solubilized in 1 N NaOH at 80 °C for 15 min and neutralized with 1 N HCl. An aliquot was removed to assess the muscle glycogen levels, and the remainder was vortexed and centrifuged at 10,000×*g* for 1 min. The aliquots were removed for scintillation counting of the [^{3}H] and [^{14}C] labels.

2.3.6. Muscle glycogen

Muscle glycogen content was assessed as previously described [31]. Briefly, aliquots of solubilized muscles from the *ex vivo* skeletal muscle glucose uptake experiments were incubated with 3.33 N HCl at 95 °C for 2 h and the samples were neutralized with 2 N NaOH and 1 M Tris–HCl pH 7.6. Hexokinase reagent (Eagle Diagnostics) was added and the reaction absorbance was read at 340 nm using a SpectraMax M4 multimode plate reader (Molecular Devices).

2.3.7. Mitochondrial respiration using high-resolution respirometry

Permeabilized muscle fiber bundles were prepared from portions of the medial gastrocnemius muscle due to its oxidative phenotype and ease of mechanical fiber separation [32,33]. Briefly, the muscles were placed in buffer X (7.23 mM K_2EGTA, 2.77 mM CaK_2EGTA, 20 mM imidazole, 20 mM taurine, 5.7 mM ATP, 14.3 mM phosphocreatine, 6.56 mM $MgCl_2$, and 50 mM K-MES, pH 7.1), and the fibers were separated using a dissecting microscope. For permeabilization, the fiber bundles were incubated in buffer X supplemented with 30 μg/ml saponin for 30 min at 4 °C. The permeabilized muscle fibers were washed in buffer Z (110 mM K-MES, 35 mM KCl, 1 mM EGTA, 5 mM K_2HPO_4, 3 mM $MgCl_26H_2O$, and 5 mg/ml bovine serum albumin, pH 7.4) at 4 °C for 15 min. The permeabilized fibers were placed in Oroboros O2K Oxygraph chambers (Oroboros Instruments) filled with buffer Z supplemented with creatine monohydrate (20 mmol/L) and 12.5 μM blebbistatin. To determine the respiratory capacity using

carbohydrate-derived substrates, the O_2 consumption rate (OCR) was measured after each sequential addition of the following: 4 mM pyruvate/0.5 mM malate/5 mM glutamate, 2.5 mM ADP, 5 mM succinate, 5 μM cytochrome c, 10 mM rotenone, 5 μM antimycin A/2 mM ascorbate, and 0.5 mM TMPD. To determine the respiratory capacity using fatty acid substrates, the OCR was measured after each sequential addition of the following: 18 μM palmitoyl-carnitine/20 μM palmitoyl-CoA/5 mM L-carnitine, 0.5 mM malate, and 1 mM ADP. Fibers were rinsed and freezer dried (Labconco, Kansas City, MO, USA). Data were normalized to the fiber dry weight.

2.3.8. Direct measurement of oxidative phosphorylation (OXPHOS) efficiency

OXPHOS efficiency was measured in permeabilized muscle fibers and isolated mitochondria via the simultaneous quantification of the ATP production and O_2 consumption (OCR) rates as previously described [32] with minor modifications. Permeabilized muscle fiber bundles were prepared as previously mentioned. Skeletal muscle mitochondria were isolated as previously described [34]. Briefly, skeletal muscle was homogenized in cold isolation media containing 0.3 M sucrose, 10 mM HEPES, 1 mM EGTA, and 1 mg/ml BSA. Homogenates were centrifuged at 800×*g* for 10 min at 4 °C. The supernatant was collected and centrifuged at 12,000×*g* for 10 min at 4 °C. The resulting pellet was resuspended with isolation media (no BSA). A final centrifugation step was performed at 12,000×*g* for 10 min at 4 °C. The final pellet was resuspended in 150 μL of isolation media. The protein concentration was determined using a Pierce BCA Protein Assay Kit (Thermo Fisher Scientific), and 12.5 μg of protein was used. Samples were placed in an Oroboros O2K Oxygraph (Oroboros Instruments) filled with buffer Z supplemented with 0.01 mM blebbistatin and 0.2 mM Ap5A. The OCR was simultaneously measured with the ATP production rate by quantification of NADPH fluorescence (excitation/emission: 340/460 nm; FluoroMax-3, Horiba Jobin Yvon, Edison, NJ, USA) at 37 °C. In this assay, ATP production was determined using an enzyme-linked assay in which the ATP hydrolyzed in a hexokinase reaction and subsequent NADPH production through the glucose-6-phosphate dehydrogenase reaction resulted in a 1:1 stoichiometry. OXPHOS flux in the permeabilized fiber bundles was measured in the presence of 0.5 mM malate/5 mM pyruvate/5 mM glutamate/10 mM succinate followed by ADP titration (20 μM, 200 μM, and 2000 μM). Data were normalized to fiber dry weight. OXPHOS efficiency (ATP/O ratio) was calculated by dividing the ATP production rate by the rate of atomic oxygen consumed.

2.3.9. Mitochondrial H_2O_2 emission potential

Mitochondrial H_2O_2 emission potential was measured fluorometrically (Fluorolog, Horiba Jobin Yvon, Edison, NJ, USA) in the permeabilized muscle fiber bundles using an Amplex Ultra Red/horseradish peroxidase detection system as previously described [35]. Briefly, fiber bundles were placed in a cuvette containing 10 μM Amplex Ultra Red, 1 mM EGTA supplemented with 25 U/mL superoxide dismutase to convert the superoxide into H_2O_2, and 25 μM blebbistatin to prevent contraction. The H_2O_2 emission rate was measured under 3 substrate conditions: 1) 10 mM succinate, 2) 37.5 μM palmitoyl-carnitine/20 μM palmitoyl-CoA/5 mM L-carnitine, and 3) 1 mM pyruvate/5 mM L-carnitine. For each assay, the H_2O_2 emission rate was also measured in the presence of 1 μM auranofin (AF), a thioredoxin reductase inhibitor, and 100 μM bis-chloroethyl nitrosourea (BCNU), a glutathione reductase inhibitor. Fluorescence was plotted against an H_2O_2 (Millipore Sigma) standard curve. Data were normalized to the fiber dry weight.

2.3.10. Muscle contractile force measurements

The extensor digitorum longus muscle (EDL) was used to assess the parameters of contractile function using a force transducer (Aurora Scientific Inc.) as previously described [36].

2.3.11. Cytokine and chemokine analysis

Blood was collected by cardiac puncture, and serum was extracted using standard methods. Cytokine and chemokine concentrations in serum samples were quantified by ELISA using a commercially available Bio-Plex Multiplex Immunoassay System kit (Bio-Rad) and read using a MAGPIX Instrument (Luminex, Austin, TX, USA) according to the manufacturer's protocol. Concentrations were calculated from standard curves using recombinant proteins and expressed in pg/mL.

2.3.12. Mitochondrial respiration measurement in human myotubes

On the fifth day of differentiation, the O_2 consumption rate (OCR) was measured using an XF24 Extracellular Analyzer and XFe96 Extracellular Analyzer according to the manufacturer's protocols. Briefly, 50,000 HSKMCs and 20,000 HSKMCs were seeded in 24- and 96-well plates, respectively. The wells were coated with 20 μg/ml ECL cell attachment matrix (Millipore Sigma). Myotubes were incubated in XF Base Medium with 1 mM pyruvate, 2 mM glutamine, and 10 mM glucose (pH 7.4) for 1 h at 37 °C in a non-CO_2 incubator. The cells were then placed into an XF Analyzer at 37 °C, and the OCR was measured after each sequential addition of the following: 1 μM oligomycin, 1 μM carbonyl cyanide-p-trifluoromethoxyphenylhydrazone (FCCP), and 0.5 μM rotenone/antimycin A. The results were normalized to the amount of protein in each well, which was quantified using the Pierce BCA Protein Assay Kit (Thermo Fisher Scientific).

2.3.13. Expression analysis by real-time quantitative PCR (RT-qPCR)

Total mRNA was extracted from the skeletal muscle of the mice using TRIzol (Invitrogen) and from the human myotubes using an RNeasy Mini Kit (Qiagen). Complementary DNA was synthesized from mRNA using a High-Capacity cDNA Reverse Transcription Kit (Applied Biosystems) according to the manufacturer's protocol. Using Quant Studio 3 (Applied Biosystems), the following TaqMan Gene Expression Assays (Thermo Fisher Scientific) were used to quantify mRNA expression: human ESR1 (Hs00174860_m1), murine ESR1 (Mm00433149_m1), murine ESR2 (Mm00599821_m1), murine TNF (Mm03928990_m1), murine IL6 (Mm00446190_m1), murine IL1b (Mm00434228_m1), murine CXCL2 (Mm 00436450_m1), murine CXCL1 (Mm04207460_m1), murine CCL2 (Mm 00441242_m1), murine CCL3 (Mm00441259_g1), human 18S (Hs99999901_s1), and murine 18S (Mm03928990_g1).

2.3.14. Immunoblotting

Immunoblotting was performed using standard methods. Proteins were extracted from tibialis anterior muscles and human myotubes with lysis buffer (.05% IGEPAL CA-630, 20 mM Tris—HCl, 150 mM NaCl, and 1 mM EDTA) supplemented with a protease inhibitor cocktail (Pierce Protease Inhibitor Tablets, Thermo Fisher Scientific). Lysates were centrifuged at 800×*g* for 15 min at 4 °C. Proteins (20—80 μg) were separated by SDS-PAGE and then transferred to PVDF or nitrocellulose membranes. Blots were probed with the primary and secondary antibodies listed in Supplementary Table S2. The blots were developed using Pierce ECL Western Blotting Substrate (Thermo Fisher Scientific) or Western Lighting Plus-ECL (PerkinElmer).

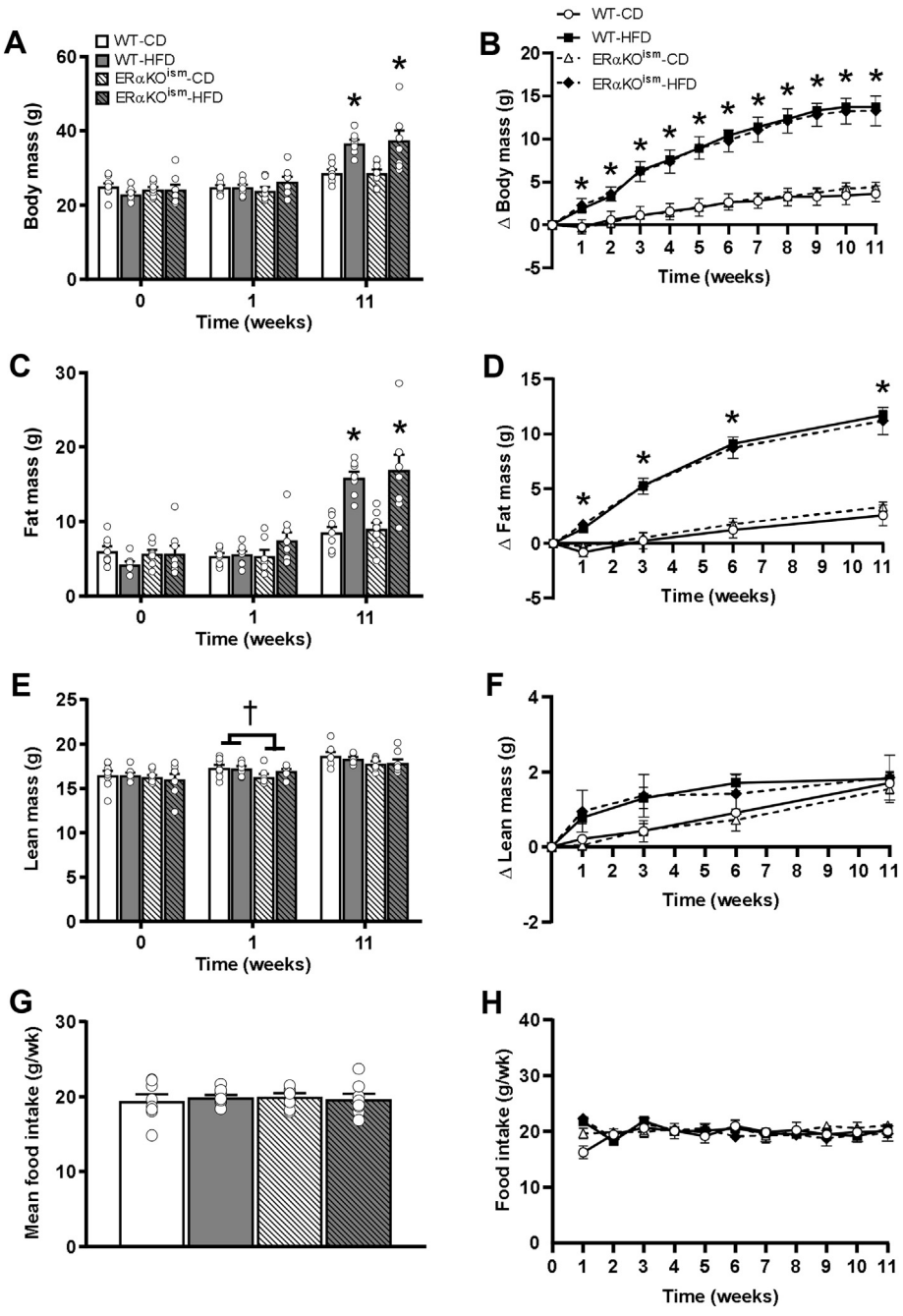

Figure 1: A–H. Induced ablation of skeletal muscle ERα in adult mice has no effect on adiposity. (A) Body mass, **(B)** change in body mass over time, **(C)** total fat mass, **(D)** change in total fat mass over time, **(E)** total lean mass, **(F)** change in total lean mass over time, **(G)** average food intake over the course of the study, and **(H)** average food intake per week of the WT and ERαKO^{ism} mice fed a control (low-fat) diet (CD) or high-fat diet (HFD). Data are mean ± SEM. *Main effect of diet, $p < .05$. †Main effect of genotype, $p < .05$. n = 8/group.

2.3.15. Two-photon microscopy and second harmonic generation

GFP-tagged ESR1-66 kDa, ESR1-46 kDa, and ESR1-36 kDa were electroporated into skeletal muscle fibers of the flexor digitorum brevis muscle as previously described [37]. Two-photon second harmonic generation was used to visualize these ESR1 isoforms with myosin and NAD/NADH autofluorescence in the skeletal muscle fibers of live mice as previously described [37]. Myosin and NAD/NADH were visualized label-free due to their unique intrinsic properties. ERα = pseudo-colored magenta, NAD/NADH = green, and myosin = red.

2.4. Statistical analysis

All the data are presented as mean ± SEM. Statistical analyses were performed using PASW Statistics 18 statistical software (Chicago, IL, USA). Two-way ANOVA was used for comparisons between the mice

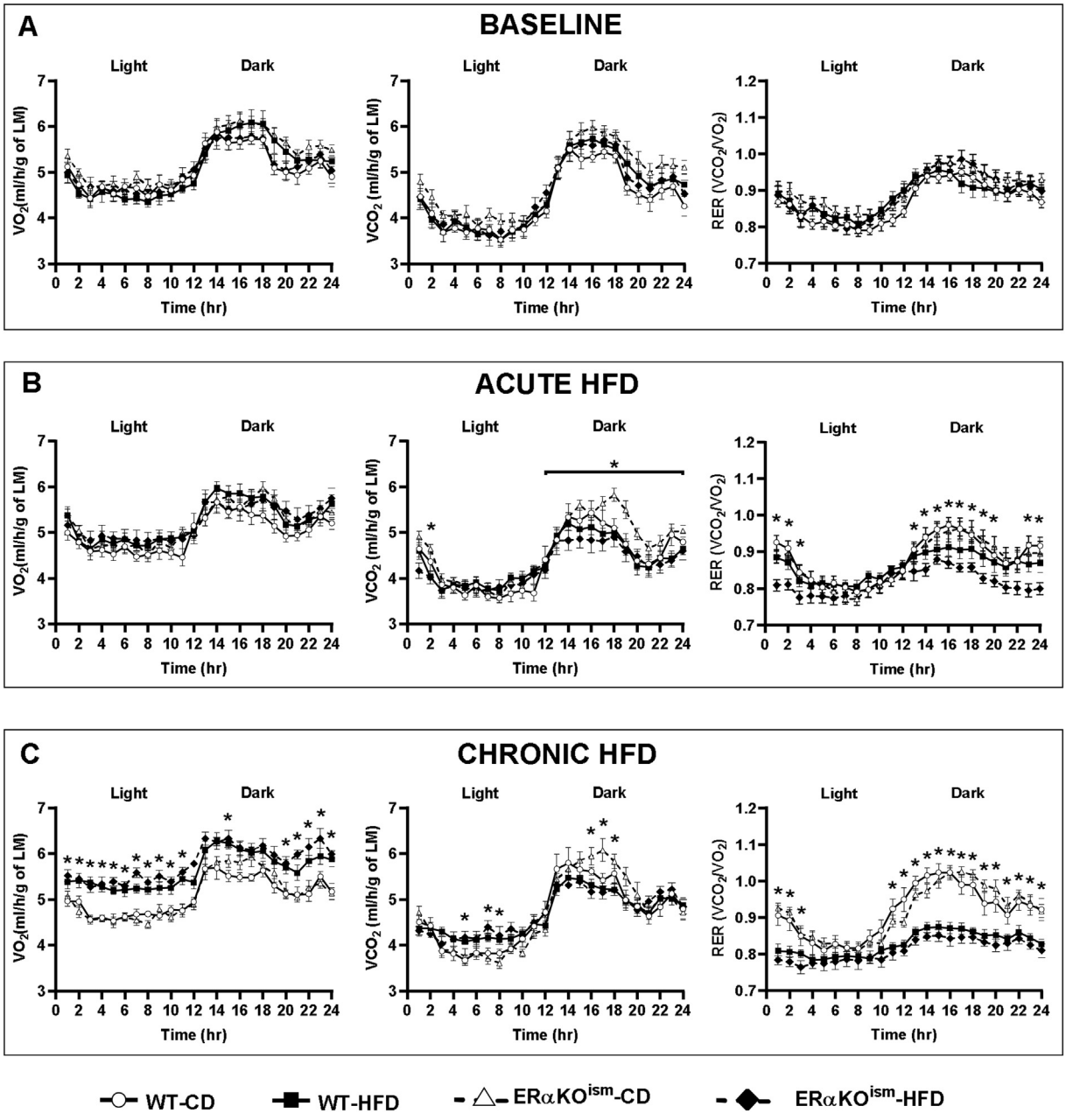

Figure 2: A–C. Induced ablation of skeletal muscle ERα in adult female mice has no effect on whole body O_2 consumption, CO_2 production, and respiratory exchange ratio. Whole body calorimeter measurements of whole body O_2 consumption (VO_2), CO_2 production (VCO_2), normalized to lean mass (LM), and respiratory exchange ratio (RER) at **(A)** baseline, **(B)** during the diet switch (first 2–3 days of week 1 HFD treatment), and **(C)** after chronic HFD. Data are mean ± SEM. *Main effect and simple main effects of diet, $p < .05$. n = 7–10/group.

that were grouped based on genotype and diet. Three-way mixed ANOVA was used to determine the group differences (genotype and diet) over time. Two-tailed independent and dependent Student's t-tests were also used when appropriate. Residual analyses were performed to test for normality, outliers, and homogeneity of variances. All of the data points/samples were included since excluding the outliers did not affect the study's overall conclusions. For all the statistical tests, $p < .05$ was considered significant. In cases in which simple 2-way interactions were determined, the Bonferroni adjustment method was used; thus, the statistically significant p-value was adjusted for the family of comparisons, dividing $p < .05$ by the number of comparisons (i.e. two simple 2-way interactions: $.05 \div 2 = .025$).

3. RESULTS

3.1. Body composition of ERαKO^{ism} mice after acute and chronic HFD

At baseline, all the groups exhibited similar body mass, fat mass, and lean mass (Figure 1A, C, and E). The change in body mass and fat mass over time was greater in the HFD-fed mice than in the CD-fed mice, but no significant differences between genotype were observed (Figure 1B,D). The absolute values of the body mass and fat mass were similar among the groups after 1 week of exposure to HFD and greater in the HFD-fed mice, regardless of genotype, after 11 weeks of exposure to HFD (Figure 1A,C). The lean mass of the

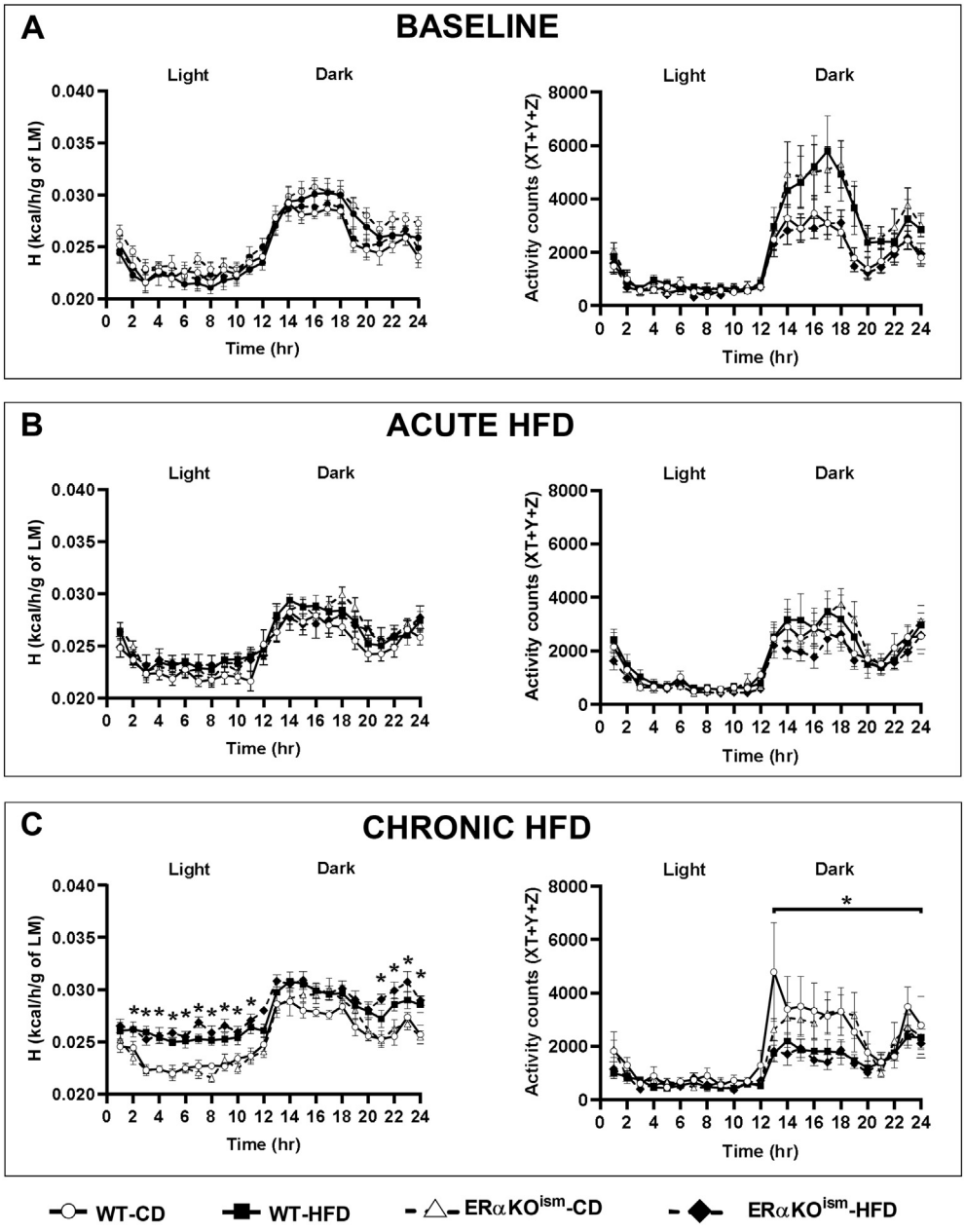

Figure 3: A–C. Induced ablation of skeletal muscle ERα in adult female mice has no effect on energy expenditure and spontaneous cage activity. Whole body calorimeter measurements of energy expenditure (H), normalized to lean mass (LM), and activity counts at **(A)** baseline, **(B)** during the diet switch (first 2–3 days of week 1 HFD treatment), and **(C)** after chronic HFD. Data are mean ± SEM. *Main effect and simple main effects of diet, $p < .05$. n = 7–10/group.

ERαKO^{ism} mice, regardless of diet, was statistically lower than in the WT mice after 1 week on HFD but not significantly different among the groups after chronic HFD treatment (Figure 1E). Food intake was similar among the groups over the course of the study (Figure 1G,H). The gonadal fat mass was greater in the HFD-fed mice, regardless of genotype, but the liver and heart masses were not affected by diet or genotype (Supplementary Table S1).

3.2. Whole body metabolic assessment during acute and chronic HFD

Indirect gas calorimetry revealed that metabolic function in the ERα KO^{ism} mice was similar to the WT mice, regardless of diet. O_2 consumption (VO_2), CO_2 production (VCO_2), respiratory exchange ratio (RER), energy expenditure (H), and activity counts were not significantly different among the groups at baseline (Figures 2A and 3A). The acute switch from the CD to the HFD (first 2–3 days of week 1 of HFD treatment) lowered VCO_2 during the dark cycle in the WT- and ERα KO^{ism}-HFD mice, which resulted in decreased RER (Figure 2B). There were no significant differences in energy expenditure and activity counts among the groups during the switch from the CD to the HFD (Figure 3B). The HFD-fed mice, regardless of genotype, exhibited lower RER during the light and dark cycles after chronic HFD treatment than the CD-fed mice (Figure 2C). The HFD-fed mice, regardless of genotype, also exhibited greater energy expenditure and lower spontaneous cage activity after chronic HFD treatment than the CD-fed mice, especially during the dark cycle (Figure 3C).

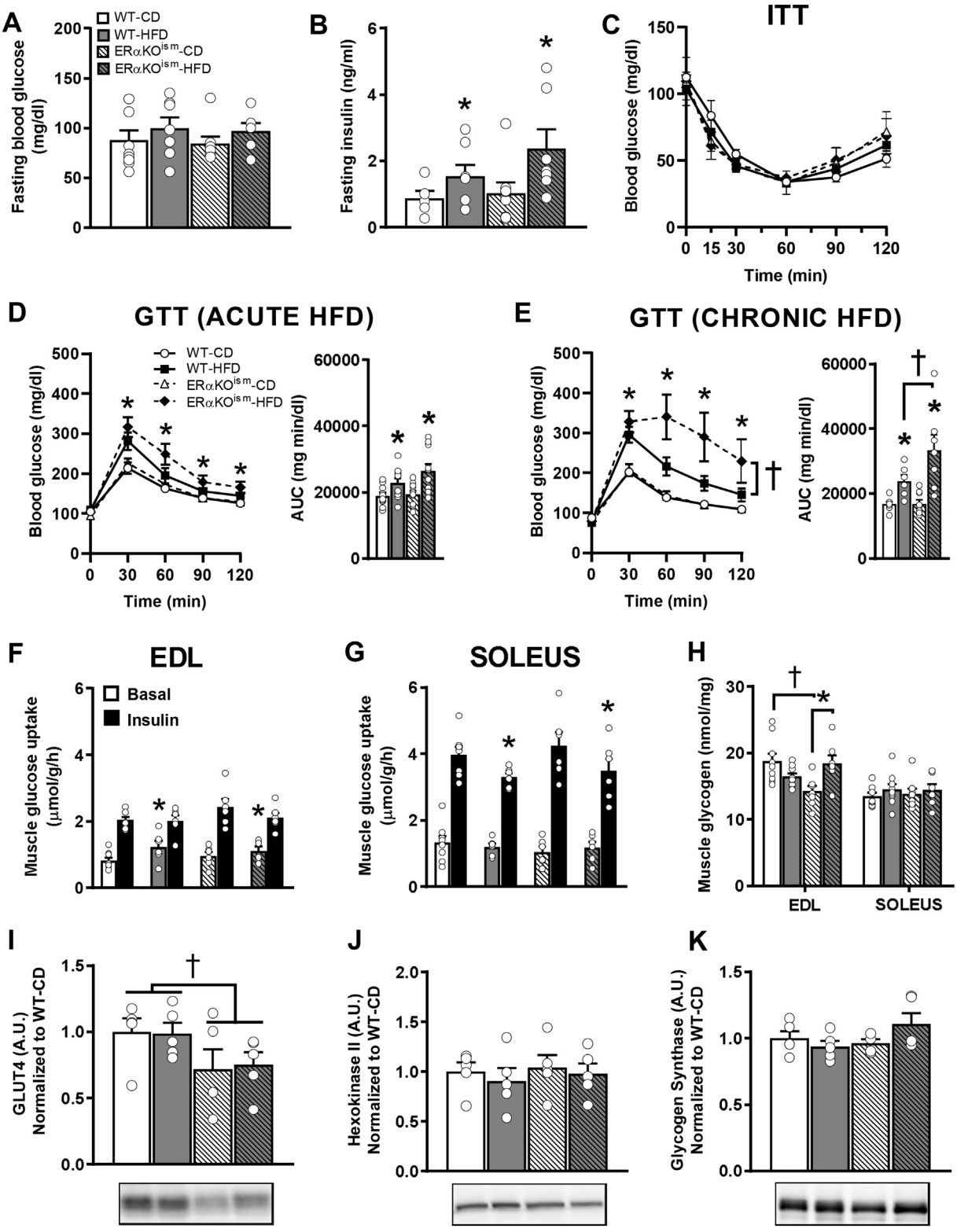

Figure 4: A-J. Induced ablation of skeletal muscle ERα in adult female mice increases the susceptibility to develop glucose intolerance after chronic HFD treatment but does not impair skeletal muscle glucose uptake. (A, B) Fasting blood glucose (n = 6–9/group) and fasting insulin after chronic (11 weeks) HFD (n = 5–8/group). **(C)** Insulin tolerance test after chronic HFD (n = 5/group). **(D, E)** Glucose tolerance after acute (1 week) HFD (n = 10–12/group) and chronic HFD (n = 6–9/group). **(F, G)** *Ex vivo* basal and insulin-stimulated skeletal muscle glucose uptake in extensor digitorum longus (EDL) and soleus muscles (n = 6–8/group), **(H)** skeletal muscle glycogen content (n = 7–9/group), and **(I–K)** immunoblots for tibialis anterior muscle protein content of glucose transporter-4 (GLUT4), hexokinase II, and glycogen synthase after chronic HFD (n = 5/group). Data are mean ± SEM. *Main effect of diet, $p < .05$. †Main and simple main effects of genotype, $p < .05$.

3.3. Glucose dynamics after acute and chronic HFD

The impact of skeletal muscle ERα ablation on glucose dynamics was assessed. Fasting blood glucose was not significantly different among the groups (Figure 4A), whereas fasting insulin was significantly higher in the HFD-fed groups after chronic HFD treatment, regardless of genotype (Figure 4B). Insulin tolerance was similar among the groups (Figure 4C). The response to a glucose bolus and the glucose area under the curve were significantly different between the CD- and HFD-fed mice after acute HFD exposure, but no significant differences between genotype were observed (Figure 4D). Interestingly, the ERα KO^{ism}-HFD mice exhibited greater glucose intolerance than the WT-HFD mice after chronic HFD exposure (Figure 4E).

Skeletal muscle glucose uptake was assessed *ex vivo* after chronic HFD treatment. Basal and insulin-stimulated glucose uptake in the extensor digitorum longus (EDL) muscle were not impaired in the ERαKO^{ism}-CD and ERαKO^{ism}-HFD mice (Figure 4F). In the soleus muscle, insulin-stimulated glucose uptake was lower in the HFD-fed mice, but there were no significant differences between genotype (Figure 4G). Muscle glycogen content after chronic HFD treatment was not significantly different among the groups in the soleus muscle. While glycogen content in the EDL muscle was significantly lower in the ERαKO^{ism}-CD mice than in the WT mice, the ERαKO^{ism}-HFD mice displayed higher muscle glycogen than the ERαKO^{ism}-CD mice, with levels similar to the WT-CD and WT-HFD mice (Figure 4H).

After chronic HFD treatment, the skeletal muscle of the ERαKO^{ism} mice exhibited lower GLUT4 protein content compared to the WT mice, regardless of diet (Figure 4I). Hexokinase and glycogen synthase protein content were similar among the groups (Figure 4J,K).

3.4. Skeletal muscle inflammation after chronic HFD

Expression of a number of pro-inflammatory cytokines and chemokines in the skeletal muscle was significantly higher in the ERαKO^{ism} mice than in the WT mice, regardless of diet (Figure 5A). Specifically, tumor necrosis factor-α (TNF-α), interleukin-6 (IL-6), chemokine (C-X-C motif) ligand 1 (CXCL1, the IL-8 homolog in mice), chemokine (C—C motif) ligand 3 (CCL3), and chemokine (C—C motif) ligand 2 (CCL2) were significantly greater in the ERαKO^{ism} mice than in the WT mice, regardless of diet (Figure 6A). Interleukin-1β (IL-1β) expression was higher in the HFD-fed mice, regardless of genotype. Chemokine (C-X-C motif) ligand 2 (CXCL2) expression was not significantly different among the groups.

In serum, the TNF-α and CCL2 concentrations were significantly lower in the ERαKO^{ism} mice than in the WT mice (Figure 5B). The CXCL2 and CXCL1 concentrations were greater only in the HFD-fed mice, regardless of genotype (Figure 6B). A panel of other cytokines and chemokines was assessed inserum, and minimal effects of skeletal muscle ERα ablation were observed (Supplementary Figures S5A—D). Although CXCL13 was significantly higher in the ERαKO^{ism}-HFD mice, CXCL12 and CXCL11 were lower in the ERαKO^{ism} mice than in the WT mice (Supplementary Figure S5A). The CCL27, CCL11, and CCL7 concentrations were higher in the HFD-fed mice, regardless of genotype (Supplementary Figure S5B). IL-4 was significantly lower in the ERα KO^{ism} mice than in the WT mice, and IL-16 was significantly greater in the HFD-fed mice, regardless of genotype (Supplementary Figure S5C). The expression levels of rest of the cytokines and chemokines in the serum were not significantly different among the groups.

3.5. Functional assessment of skeletal muscle mitochondria *in situ* after chronic HFD

ERα is thought to play a prominent role in regulating mitochondrial function; thus, mitochondrial respiration kinetics were assessed in

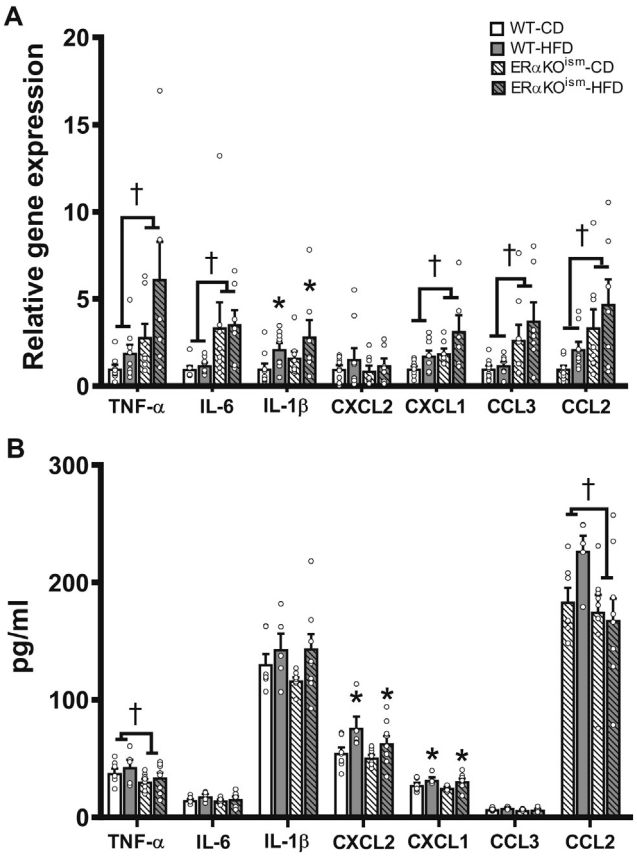

Figure 5: Induced ablation of skeletal muscle ERα in adult female mice alters inflammatory markers in skeletal muscle, but not in systemic circulation. Key inflammatory cytokines and chemokines in **(A)** gastrocnemius (n = 7—9/group) and **(B)** blood serum of WT and ERαKO^{ism} mice after chronic HFD (n = 5—9/group). mRNA expression was measured by RT-qPCR and normalized to 18s rRNA. TNF-α = tumor necrosis factor-α; IL-6 = interleukin-6; IL-1β = interleukin-1β; CXCL2 = chemokine (C-X-C motif) ligand 2; CXCL1 = chemokine (C-X-C motif) ligand 1; CCL3 = chemokine (C—C motif) ligand 3; chemokine (C—C motif) ligand 2. Data are means ± SEM. *Main effect of diet, $p < .05$. †Main effect of genotype, $p < .05$.

permeabilized skeletal muscle fiber bundles across all of the groups at the 12-week time point. The ADP-stimulated rate of O_2 consumption (JO_2) during respiration supported by pyruvate/malate/glutamate was similar in the permeabilized fiber bundles of the ERαKO^{ism} mice vs the WT mice, regardless of diet; however, an increase in Complex IV-supported respiration was observed in fiber bundles of the WT-HFD mice compared to the WT-CD mice (Figure 6A). Maximal ADP-stimulated JO_2 during fatty acid-supported respiration (in the presence of palmitoyl-carnitine/palmitoyl-CoA) was similar among all of the groups (Figure 6B). The rates of ATP production (JATP) and JO_2 were also simultaneously measured to determine OXPHOS efficiency (defined as the molar amount of ATP produced per mole of atomic oxygen consumed (ATP/O ratio)) in the skeletal muscle. The ATP/O ratio in the permeabilized fiber bundles was not significantly different across all the groups (Figure 6C). ATP/O in the isolated skeletal muscle mitochondria was also similar among the groups (Supplementary Figure S6A). In line with our findings on mitochondrial ATP production and OXPHOS efficiency, the contractile force and fatigue susceptibility were not affected in the ERαKO^{ism} mice, regardless of diet (Supplementary Figures S7A—C).

The permeabilized fiber bundles of the ERαKO^{ism} mice did not exhibit any significant differences in the H_2O_2 emitting potential in the

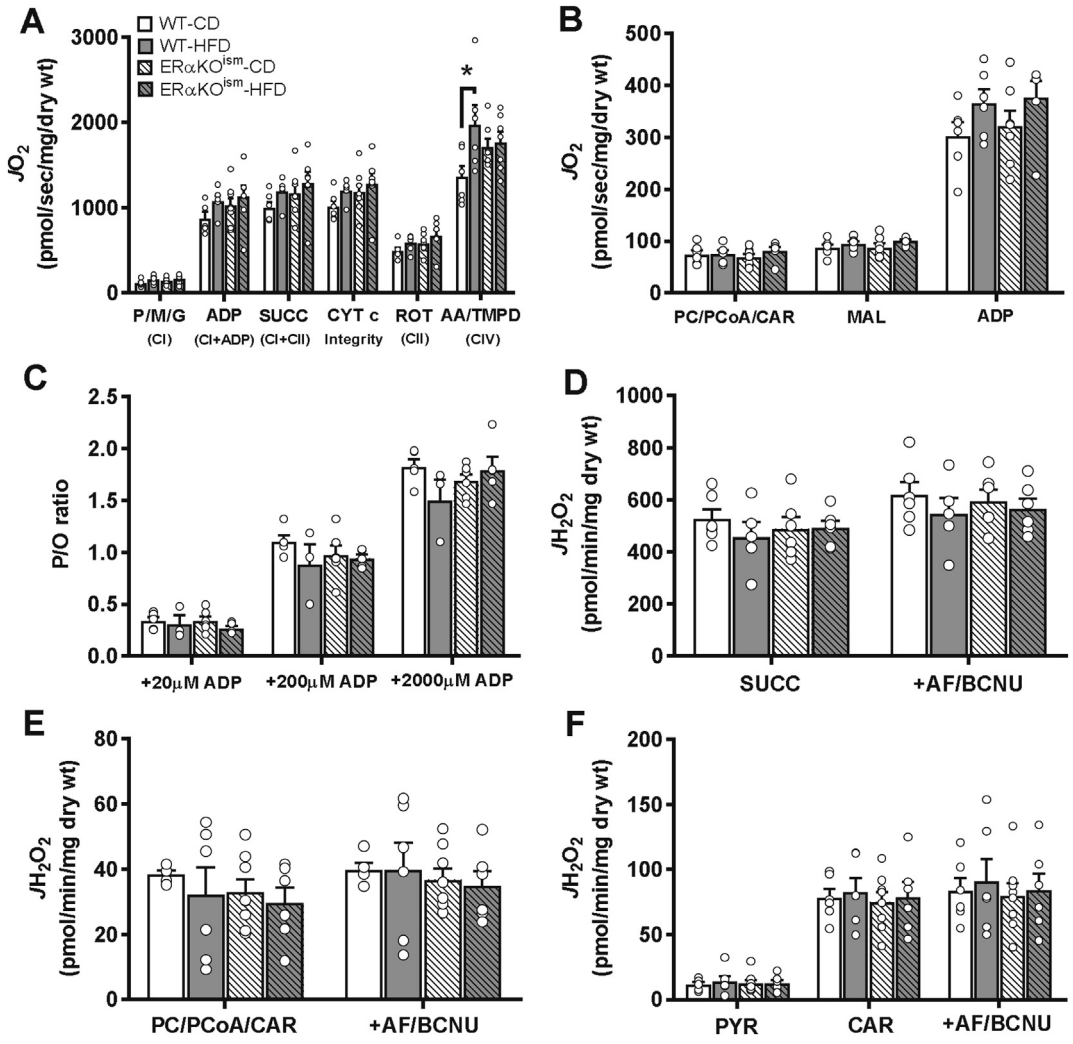

Figure 6: A–F. Induced ablation of skeletal muscle ERα in adult mice does not adversely affect mitochondrial respiratory capacity, OXPHOS efficiency, and H_2O_2 emitting potential. (A) Pyruvate (P)/malate (M)/glutamate (G)-supported oxygen consumption rate (JO_2) (n = 6–8/group). **(B)** Palmitoyl-carnitine (PC)/palmitoyl-CoA (PCoA)/L-carnitine (Car)-supported JO_2 (n = 6–7/group). **(C)** OXPHOS efficiency (ATP/O ratio) (n = 3–6/group). **(D)** H_2O_2 emission rates in permeabilized muscle fibers of WT and ERαKO^{ism} mice in the presence of succinate (SUCC) (n = 5–6/group), **(E)** palmitoyl-carnitine (PC)/palmitoyl-CoA (PCoA)/L-carnitine (CAR) (n = 5–8/group), and **(F)** pyruvate (PYR)/carnitine (CAR) (n = 6–8/group) and after subsequent addition of auranofin/bis-chloroethyl nitrosourea (AF/BCNU). CI=Complex I; CII=Complex II; CI + II=Complex I + Complex II; CIV=Complex IV; ADP = adenosine diphosphate; CYT c = cytochrome c; ROT = rotenone; AA = antimycin A; Asc = ascorbate; TMPD = N,N,N′,N′-tetramethyl-p-phenylenediamine dihydrochloride; H_2O_2 = hydrogen peroxide; wt = weight. Data are mean ± SEM. *Simple main effect of diet, $p < .05$.

presence of succinate (Figure 6D), palmitoyl-carnitine/palmitoyl-CoA (Figure 6E), or pyruvate/carnitine (Figure 6F) compared to their WT counterparts, regardless of diet. As expected, JH_2O_2 production in the presence of AF/BCNU was greater under all substrate conditions with no differences among the groups (Figure 6D–F).

3.6. Mitochondrial respiration in human myotubes with reduced ERα function

To reconcile our findings on mitochondrial function with a previous publication that demonstrated a large loss of respiratory function with ERα ablation [20], we measured mitochondrial respiration in human myotubes with significantly reduced ERα. Myotubes were cultured from primary human skeletal muscle cells isolated from muscle biopsies of healthy and obese insulin-resistant (OIR) young adult women. The OIR women exhibited greater body weight, body mass index, fasting insulin levels, HOMA-IR, and lower maximal O_2 consumption (VO_2max) compared to the healthy women (Table 1). ESR1 (ERα) mRNA expression in the myotubes was not significantly different between the healthy and OIR groups (Figure 7A). The myotubes were transduced with an adenovirus expressing RFP-tagged ERαshRNA (ERαKD) or RFP-tagged scrambled shRNA (Scr). The transduction

Table 1 – Subject characteristics.

	Healthy	Obese Insulin-Resistant
Sample size (N)	9	5
Age (y)	24 ± 1.6	41 ± 3.6*
Weight (kg)	62.1 ± 2.0	113.0 ± 5.3*
BMI (kg/m^2)	22.9 ± 0.8	41.0 ± 1.8*
Insulin (mU/L)	5.4 ± 0.6	15.3 ± 1.5*
Glucose (mg/dl)	86.0 ± 2.6	96.4 ± 4.3
HOMA IR	1.2 ± 0.1	3.7 ± 0.5*
VO_2max (ml/kg/min)	44.9 ± 1.6	23.0 ± 1.8*

Data are mean ± SEM. *Significant difference ($p < .05$).

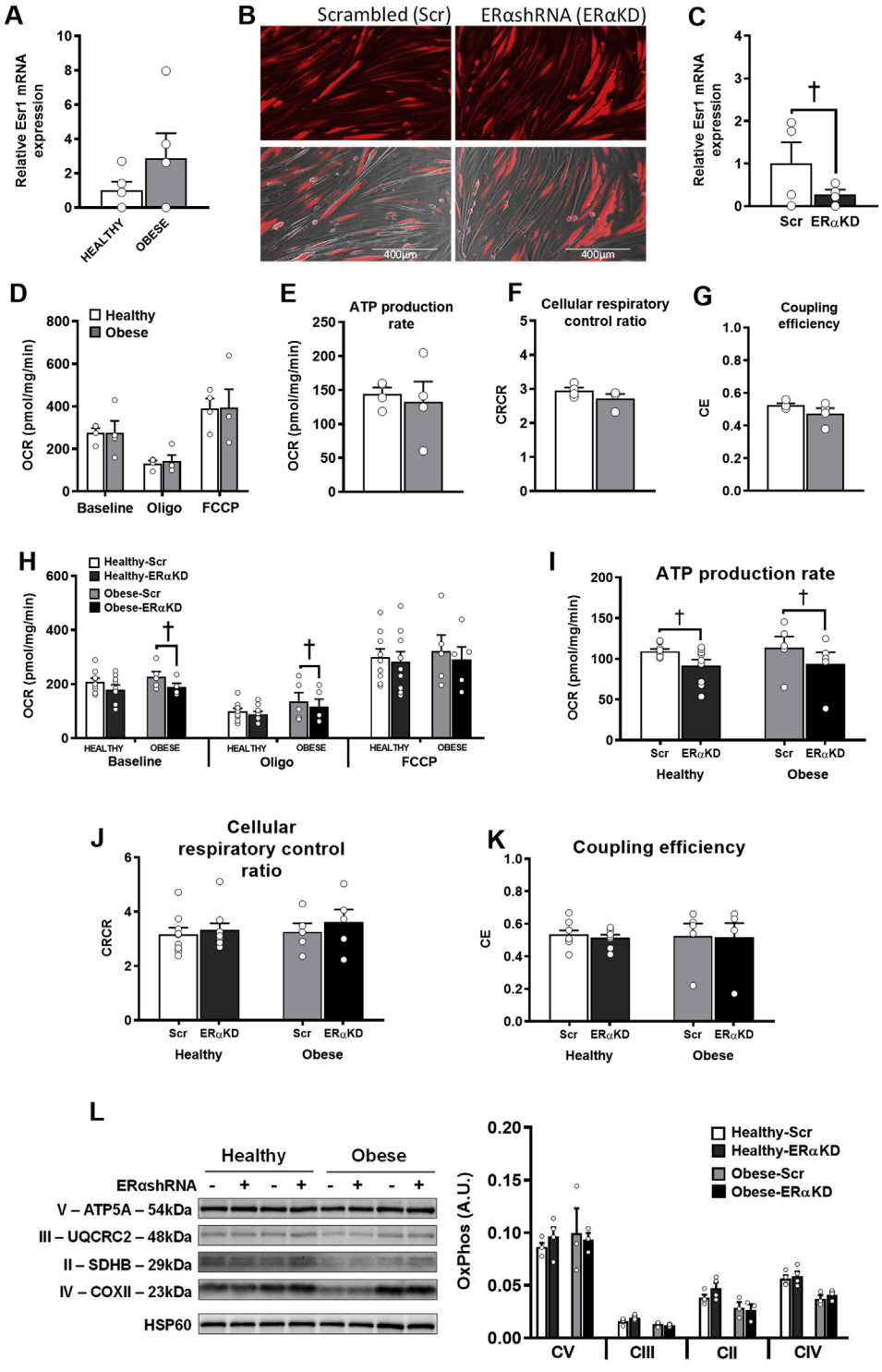

Figure 7: A–L. Knockdown of ERα in human myotubes from healthy and obese insulin-resistant women minimally affects basal O_2 consumption and ATP production rates. (A) Relative ESR1 mRNA expression in human myotubes from healthy and obese insulin-resistant groups (n = 5/group). **(B)** Representative fluorescent images of human myotubes transduced with either RFP-tagged scrambled shRNA or ERαshRNA adenovirus. **(C)** ESR1 expression in control (scrambled, Scr) and ERα knockdown (ERαKD) myotubes (n = 4/group). **(D)** O_2 consumption rate (OCR). **(E)** ATP production rate. **(F)** Cellular respiratory control ratio. **(G)** Coupling efficiency of healthy and obese insulin-resistant myotubes (n = cultured myotubes from 4 women/group, 5–6 technical replicates/condition). **(H)** O_2 consumption rate (OCR). **(I)** ATP production rate. **(J)** Cellular respiratory control ratio. **(K)** Coupling efficiency of healthy and obese insulin-resistant Scr and ERαKD myotubes (n = cultured myotubes from 5 to 9 women/group, 8–10 technical replicates/condition). **(L)** Immunoblotting for protein content of OXPHOS subunits normalized to heat shock protein 60 (HSP60) (n = 3–4/group). Oligo = oligomycin; FCCP = carbonyl cyanide-p-trifluoromethoxyphenylhydrazone; CRCR = cellular respiratory control ratio; CII=Complex II; CIII=Complex III; CIV=Complex IV; CV=Complex V. Data are mean ± SEM. †Significant difference between scrambled shRNA and ERαshRNA, $p < .05$.

efficiency was similar between the Scr and ERαKD myotubes (Figure 7B). RT-qPCR revealed that ESR1 mRNA was significantly reduced in ERα knockdown (ERαKD) myotubes compared to the Scr control (Figure 7C). Mitochondrial respiration as assessed by the oxygen consumption rates (OCR) was not significantly different between the healthy and OIR-Scr myotubes (Figure 7D). In myotubes from the healthy subjects, only the ATP production rate was minimally reduced by 16% in the ERαKD group compared to the Scr group (Figure 7I). The ERαKD myotubes from the OIR subjects exhibited a slightly lower basal O_2 consumption rate (∼16%) compared to the Scr condition and a lower ATP production rate to some extent (∼18%) (Figure 7H,I). No significant differences in the uncoupled oxygen consumption rate were found between the Scr and ERαKD myotubes from either the healthy or obese groups (Figure 7J,K). These results were not due to alterations in the protein content of the electron transport system complexes (Figure 7L).

4. DISCUSSION

Emerging evidence suggests that ERα in skeletal muscle is critical for maintaining skeletal muscle insulin sensitivity and mitochondrial respiratory function [19,20]. However, these conclusions were derived using global ERαKO mice [19,38,39] and conventional skeletal muscle-specific ERα knockout models [20], both of which have ERα ablated from skeletal muscle during prenatal and postnatal stages of development. It is unclear whether deletion of ERα during either stage of development significantly impacts the resulting phenotype of the skeletal muscle in adults. To overcome this potential concern, we generated an ERα knockout mouse model in which ERα deletion in the skeletal muscle was induced after the mice reached adulthood. Our results demonstrate that the ablation of ERα in the skeletal muscle of adult female mice does not result in any differences in *ex vivo* insulin-induced glucose uptake in the skeletal muscle or alterations in mitochondrial respiratory capacity. In addition, knockdown of ERα in human myotubes results in small changes in mitochondrial respiratory function, suggesting that ERα is not required to maintain mitochondrial capacity in adults. The ERαKO^{ism} mice, regardless of diet, exhibited elevations in mRNA levels in a number of pro-inflammatory cytokines (TNF-α, IL-6, and chemokines CCL2 and CCL3) compared to the WT mice; however, none of these were elevated in the serum. Collectively, these data suggest that induced ablation of skeletal muscle-specific ERα in adult female mice does not recapitulate the same degree of metabolic changes that global ERαKO or MERKO mice exhibit.

The ability of the mitochondria to regulate energy charge and redox potential has a significant influence on muscle insulin sensitivity [40,41]. Specifically, insulin resistance can develop due to overproduction of H_2O_2 by the mitochondria that occurs as a result of increased pressure from chronic overnutrition [40,41], resulting in a shift in the redox environment that attenuates the insulin-signaling response [41]. Recent evidence suggests that ERα regulates the metabolic function of skeletal muscle via direct regulation of mitochondria dynamics [20]. In non-muscle tissue, ERα regulates mitochondrial function by influencing mitochondrial DNA-encoded gene transcription through ER element-like consensus sequences found in several genes in the Complex I–V subunits of the electron transport system [42]. In skeletal muscle, MERKO mice exhibit a reduction in insulin sensitivity that is associated with reduced mitochondrial fission, fusion dynamics, and mitochondrial calcium retention capacity [20]. In addition, using indirect measures of ROS emission, MERKO mice appear to have disruptions in ROS regulation, suggesting that ERα is critical for mitochondrial regulation in skeletal muscle [20]. However, our data collected in the ERαKO^{ism} mice contradict this concept. Specifically, we found no differences in the respiration kinetics between the ERαKO^{ism} and WT mice when using fiber bundles to assess complex specific-driven mitochondrial respiration. Furthermore, we found no genotype differences when assessing mitochondrial efficiency (ATP/O ratio) in the fiber bundles; however, we found trends for differences in the same measure when using isolated mitochondria, which may suggest that the preparation had an effect on the outcome. Since the mitochondrial structure was maintained in the fiber bundle preparation, we feel it was a better representation of the *in vivo* environment. We also did not find differences in the H_2O_2 emitting potential between the genotypes. Thus, our data suggest that genetic ablation of ERα in the skeletal muscle of adult female mice does not affect skeletal muscle mitochondrial function.

To explain the differences between our data and the mitochondrial respiration data presented in Ribas et al. (2016) [20], we assessed the effects of ERα knockdown in cultured myotubes from human subjects. The reason we chose primary human muscle cells as a model was predicated by the fact that we found C2C12 myotubes to have extremely low ERα mRNA expression compared to adult skeletal muscle (∼600-fold difference compared to whole gastrocnemius) (see Figure S2B). Ribas et al. (2016) found that basal and maximal respiratory capacity, ATP synthesis, and palmitate oxidation rate were drastically (∼50%) lower in C2C12 myotubes transduced with ERαshRNA compared to scrambled shRNA myotubes [20]. In contrast, we found that ERα knockdown in human myotubes isolated from adult healthy and obese insulin-resistant women resulted in minimal effects on OCR, which is unlikely to be physiologically meaningful as the calculated ATP production rates were largely unaffected by ERα knockdown (only ∼16–18% in the healthy and OIR ERαKD groups). Together, the data suggest that the induced deletion of ERα in adult animals or human muscle cells has a minimal impact on mitochondrial respiratory function.

The collective literature clearly indicates that decreases in circulating estrogens through ovary removal negatively impact skeletal muscle metabolic function [34,43–45]. Thus, our data suggest that in adult animals, estrogens may impact skeletal muscle metabolism through multiple mechanisms that are independent of ERα. Estrogen treatment of the skeletal muscle of ERαKO^{ism} *ex vivo* might reveal estrogen effects on glucose metabolism and mitochondrial function independent of ERα; however, this remains to be investigated. In support of this argument, we recently found that 17β-estradiol localizes to the mitochondrial membrane in which it lowers membrane microviscosity and facilitates bioenergetic function in an ERα-independent fashion [34]. This hypothesis concurs with other previous findings suggesting that estrogens can act independent of ERs to alter cell function; however, this idea needs further examination.

Our findings are largely in contrast to previous studies that documented that global ERαKO and conventional skeletal muscle-specific ERαKO (MERKO) mice on a control (low-fat) diet displayed greater gonadal adiposity, systemic and local skeletal muscle insulin resistance, and altered mitochondrial respiration [19,20,38,39]. Given that global ERαKO and MERKO mice (which are built using muscle creatine kinase promoter to drive Cre expression) are generated in a manner in which ERα function is ablated during the early stages of development (within weeks of conception), the disparity between our data and previous findings suggest that ERα is essential for establishing the metabolic phenotype of skeletal muscle that exists in adult muscle later in life, but not nearly as critical for maintaining metabolic function post-development. Several lines of evidence support this observation. First, estrogens are known to play major roles in cell proliferation and

organ differentiation during fetal development [46,47], including skeletal muscle [48]. Further, skeletal muscle development during the transition from the late fetal period to 1−3 days post-partum exhibits significant increases in muscle oxidative capacity induced by the upregulation of a multitude of genes, including those that contain ERα cis-regulatory motifs [48]. In addition, mitochondria undergo dramatic remodeling in the first 6 weeks of postnatal muscle development, including significant changes in the total levels of OXPHOS protein content [49]. Thus, it is reasonable to speculate that differences between the MERKO and ERαKO^{ism} mice could be explained by the idea that skeletal muscle ERα is critical for mediating estrogen function during fetal developmental programming or for mitochondrial remodeling that occurs during postnatal muscle development [19,20]. This is not an unreasonable explanation given that E2 levels peak immediately after birth then return to baseline before rising again with the initiation of the estrous cycle. Thus, the skeletal muscle of MERKO mice fails to experience an E2 surge due to the loss of ERα, whereas ERα deletion in ERαKO^{ism} mice does not occur until adulthood, after postnatal development is complete. Other researchers previously proposed that such mechanisms may explain disparities between loss-of-function since birth and induced loss-of-function in adult mice [25,50]. Thus, it is possible that the increase in E2 levels immediately after birth and during postnatal growth are critical for establishing the phenotype of skeletal muscle, and the deletion of ERα after these events does not result in the same metabolic derangements seen in MERKO mice that lack ERα at birth.

The findings also suggest that ERα may play a role in preventing local inflammation in skeletal muscle; however, whether the influx of inflammatory cells into muscle is altered in ERαKO^{ism} and its impact on skeletal muscle metabolic function remains to be determined. Inflammation remains specific to skeletal muscle as no elevations in serum pro-inflammatory cytokines were found between genotypes; however, it is critical that follow-up experiments attempt to identify inflammatory cell identity within the muscle. Similar findings have been reported using other models and tissues. For example, reduced circulating estrogens by ovariectomy results in greater expression of intra-abdominal adipose pro-inflammatory markers CCL2, F4/80, CD11c, IL-12p40, and IFN-γ than sham-operated mice [51]. In addition, global ERαKO and conventional skeletal muscle-specific ERαKO (MERKO) mice exhibit elevated expression of pro-inflammatory markers, TNF-α, and p-JNK in skeletal muscle [19,20]. The accumulation of local skeletal muscle pro-inflammatory factors is known to exert paracrine effects that can decrease insulin signaling and glucose uptake [52]. Surprisingly, although ERαKO^{ism} exhibits HFD-induced glucose intolerance and signs of localized muscle inflammation, *ex vivo* skeletal muscle glucose uptake was similar between ERαKO^{ism} and WT mice, suggesting that glucose intolerance is not simply explained by skeletal muscle insulin resistance.

ERα expression is relatively low in skeletal muscle compared to other estrogen-sensitive tissues, raising the possibility that ERα is simply not critical to the regulation of metabolism in adult muscle. In fact, using a unique mouse model that harbors a synthetic multimer of canonical EREs that drive expression of the luciferase gene, Ciana et al. (2001) [53] demonstrated that skeletal muscle was one of the lowest estrogen-responsive tissues in the entire mouse. To date, much of our understanding of ERα and estrogens has been determined using mice (that is, OVX, ARKO, and ERKO) that develop numerous secondary characteristics that can influence primary research results. As previously speculated, it is possible that ER-independent mechanisms [34] can compensate for loss ERα function in adult animals. Thus, it is also possible and should be considered that genomic signaling driven by ERα does not play a major role in skeletal muscle. However, a caveat that should be considered is the interaction with age, since risk of insulin resistance increases with age. In these experiments, all the animals were tested as adults; however, it is unclear if the same results would occur if aged (>12 mos) animals were tested, so critical follow-up studies are necessary.

5. CONCLUSIONS

Collectively, our data suggest that skeletal muscle ERα in adult female mice contributes to the maintenance of glucose tolerance under chronic lipid overload. However, it is not required for skeletal muscle glucose uptake, the regulation of basal insulin levels, mitochondrial respiration, oxidative phosphorylation efficiency, or ROS regulation. These findings differ from global and conventional skeletal muscle-specific ERαKO studies, which suggest that adaptive or redundant mechanisms are likely established by the time ERα function is lost in adult skeletal muscle. Finally, it is necessary to consider non-canonical functions of estrogens in tissues such as skeletal muscle as a means of physiological and metabolic regulation.

FUNDING

This study was supported by grant funding from ADA 1-15-BS-170 (E.E.S.), NIH RO1AR066660 (E.E.S.), NIH RO1HL125695 (J.M.M.), NIH RO1DK107397 (K.F.), NIH RO3DK109888 (K.F.), F32DK109556 (T.D.H.), NIH RO1AG031743 (D.A.L.), NIH RO1DK096907 (P.D.N.), NIH RO1DK103562 (C.A.W.), and NIH RO1GM29090 (L.A.L.).

AUTHOR CONTRIBUTIONS

Conceptualization: E.E.S., M.R.I., D.A.L., and P.D.N. Methodology: E.E.S., K.C.J., L.A.L., D.A.L., T.D.H., and K.F. Investigation: M.R.I., A.J.A., M.D.T., N.P.B., K.G.J., D.J.P., K.C.J., M.J.T., C.L., C.D.S., C.A.W., S.L.M., L.A.W., E.C.S., B.B.K.B., S.W.R., and C.E.P. Funding acquisition: E.E.S. Writing, review, and editing: M.R.I., M.D.T., M.J.T., L.A.L., D.A.L., C.A.W., J.M.M., P.D.N., and E.E.S. Resources: E.E.S., J.M.M., L.A.L., T.D.H., and K.F. Supervision: E.E.S.

ACKNOWLEDGMENTS

The authors thank Dr. K. Korach for supplying the ERα$^{flox/flox}$. Special thanks to Dr. A. Hevener for helping secure the mice.

CONFLICT OF INTEREST

The authors declare that they have no known competing financial interests or personal relationships that could have appeared to influence the work reported in this paper.

APPENDIX A. .SUPPLEMENTARY DATA

Supplementary data to this article can be found online at https://doi.org/10.1016/j.molmet.2019.12.010.

REFERENCES

[1] Park, Y.W., Zhu, S., Palaniappan, L., Heshka, S., Carnethon, M.R., Heymsfield, S.B., 2003. The metabolic syndrome: prevalence and associated risk factor findings in the US population from the third national health and

nutrition examination survey, 1988-1994. Archives of Internal Medicine 163(4): 427–436.
[2] Carr, M.C., 2003. The emergence of the metabolic syndrome with menopause. Journal of Clinical Endocrinology & Metabolism 88(6):2404–2411.
[3] Pu, D., Tan, R., Yu, Q., Wu, J., 2017. Metabolic syndrome in menopause and associated factors: a meta-analysis. Climacteric 20(6):583–591.
[4] Lo, J.C., Zhao, X., Scuteri, A., Brockwell, S., Sowers, M.R., 2006. The association of genetic polymorphisms in sex hormone biosynthesis and action with insulin sensitivity and diabetes mellitus in women at midlife. The American Journal of Medicine 119(9 Suppl 1):S69–S78.
[5] Salpeter, S.R., Walsh, J.M., Ormiston, T.M., Greyber, E., Buckley, N.S., Salpeter, E.E., 2006. Meta-analysis: effect of hormone-replacement therapy on components of the metabolic syndrome in postmenopausal women. Diabetes, Obesity and Metabolism 8(5):538–554.
[6] McCarthy, A.M., Menke, A., Visvanathan, K., 2013. Association of bilateral oophorectomy and body fatness in a representative sample of US women. Gynecologic Oncology 129(3):559–564.
[7] Ahtiainen, M., Alen, M., Pöllänen, E., Pulkkinen, S., Ronkainen, P.H.A., Kujala, U.M., et al., 2012. Hormone therapy is associated with better body composition and adipokine/glucose profiles: a study with monozygotic co-twin control design. Menopause 19(12):1329–1335.
[8] Ziel, H.K., Finkle, W.D., 1975. Increased risk of endometrial carcinoma among users of conjugated estrogens. New England Journal of Medicine 293(23): 1167–1170.
[9] Anderson, G., Limacher, M., Assaf, A., Bassford, T., Beresford, S., Black, H., et al., 2004. Effects of conjugated equine estrogen in postmenopausal women with hysterectomy: the Women's Health Initiative randomized control trial. The Journal of the American Medical Association 291(14):1701–1712.
[10] Rossouw, J.E., Anderson, G.L., Prentice, R.L., LaCroix, A.Z., Kooperberg, C., Stefanick, M.L., et al., 2002. Risks and benefits of estrogen plus progestin in healthy postmenopausal women: principal results from the Women's Health Initiative randomized controlled trial. The Journal of the American Medical Association 288(3):321–333.
[11] Pinkerton, J.A.V., Aguirre, F.S., Blake, J., Cosman, F., Hodis, H., Hoffstetter, S., et al., 2017. The 2017 hormone therapy position statement of the North American Menopause Society. Menopause 24(7):728–753.
[12] Manson, J.A.E., Chlebowski, R.T., Stefanick, M.L., Aragaki, A.K., Rossouw, J.E., Prentice, R.L., et al., 2013. Menopausal hormone therapy and health outcomes during the intervention and extended poststopping phases of the women's health initiative randomized trials. The Journal of the American Medical Association 310(13):1353–1368.
[13] Couse, J., Lindzey, J., Grandien, K., Gustafsson, J., Korach, K., 1997. Tissue distribution and quantitative analysis of estrogen receptor-alpha (ERalpha) and estrogen receptor-beta (ERbeta) messenger ribonucleic acid in the wild-type and ERalpha-knockout mouse. Endocrinology 138(11):4613–4621.
[14] Kuhl, H., 2005. Pharmacology of estrogens and progestogens: influence of different routes of administration. Climacteric 8(SUPPL. 1):3–63.
[15] Barros, R., Gustafsson, J.-Å., 2011. Estrogen receptors and the metabolic network. Cell Metabolism 14(3):289–299.
[16] Hevener, A.L., Clegg, D.J., Mauvais-Jarvis, F., 2015. Impaired estrogen receptor action in the pathogenesis of the metabolic syndrome. Molecular and Cellular Endocrinology 418(3):306–321.
[17] Klinge, C.M., 2001. Estrogen receptor interaction with estrogen response elements. Nucleic Acids Research 29(14):2905–2919.
[18] Driscoll, M.D., Sathya, G., Muyan, M., Klinge, C.M., Hilf, R., Bambara, R.a., 1998. Sequence requirements for estrogen receptor binding to estrogen response elements. Journal of Biological Chemistry 273(45):29321–29330.
[19] Ribas, V., Nguyen, M.T.A., Henstridge, D.C., Nguyen, A.-K., Beaven, S.W., Watt, M.J., et al., 2010. Impaired oxidative metabolism and inflammation are associated with insulin resistance in ERalpha-deficient mice. American Journal of Physiology - Endocrinology And Metabolism 298(2):E304–E319.
[20] Ribas, V., Drew, B.G., Zhou, Z., Phun, J., Kalajian, N.Y., Soleymani, T., et al., 2016. Skeletal muscle action of estrogen receptor alpha is critical for the maintenance of mitochondrial function and metabolic homeostasis in females. Science Translational Medicine 8(334):1–21.
[21] Baltgalvis, K.A., Greising, S.M., Warren, G.L., Lowe, D.A., 2010. Estrogen regulates estrogen receptors and antioxidant gene expression in mouse skeletal muscle. PLoS One 5(4):e10164.
[22] Heine, P.A., Taylor, J.A., Iwamoto, G.A., Lubahn, D.B., Cooke, P.S., 2000. Increased adipose tissue in male and female estrogen receptor-alpha knockout mice. Proceedings of the National Academy of Sciences 97(23): 12729–12734.
[23] Bryzgalova, G., Gao, H., Ahren, B., Zierath, J.R., Galuska, D., Steiler, T.L., et al., 2006. Evidence that oestrogen receptor-α plays an important role in the regulation of glucose homeostasis in mice: insulin sensitivity in the liver. Diabetologia 49(3):588–597.
[24] Ohlsson, C., Hellberg, N., Parini, P., Vidal, O., Bohlooly-Y, M., Rudling, M., et al., 2000. Obesity and disturbed lipoprotein profile in estrogen receptor-alpha-deficient male mice. Biochemical and Biophysical Research Communications 278(3):640–645.
[25] Qiu, S., Vazquez, J.T., Boulger, E., Liu, H., Xue, P., Hussain, M.A., et al., 2017. Hepatic estrogen receptor α is critical for regulation of gluconeogenesis and lipid metabolism in males. Scientific Reports 7(1661): 1–12.
[26] Matic, M., Bryzgalova, G., Gao, H., Antonson, P., Humire, P., Omoto, Y., et al., 2013. Estrogen signalling and the metabolic syndrome: targeting the hepatic estrogen receptor alpha action. PLoS One 8(2):e57458.
[27] Lyons, G., Muhlebach, S., Moser, A., Masood, R., Paterson, B., Buckingham, M., et al., 1991. Developmental regulation of creatine-kinase gene-expression by myogenic factors in embryonic mouse and chick skeletal-muscle. Development 113(3):1017–1029.
[28] McCarthy, J.J., Srikuea, R., Kirby, T.J., Peterson, C.A., Esser, K.A., 2012. Inducible Cre transgenic mouse strain for skeletal muscle-specific gene targeting. Skeletal Muscle 2(1):1–7.
[29] Jackson, K.C., Tarpey, M.D., Valencia, A.P., Iñigo, M.R., Pratt, S.J., Patteson, D.J., et al., 2018. Induced Cre-mediated knockdown of Brca1 in skeletal muscle reduces mitochondrial respiration and prevents glucose intolerance in adult mice on a high-fat diet. Federation of American Societies for Experimental Biology Journal 32:1–15.
[30] McMillin, S.L., Schmidt, D.L., Kahn, B.B., Witczak, C.A., 2017. GLUT4 is not necessary for overload-induced glucose uptake or hypertrophic growth in mouse skeletal muscle. Diabetes 66(6):1491–1500.
[31] Witczak, C.A., Hirshman, M.F., Jessen, N., Fujii, N., Seifert, M.M., Brandauer, J., et al., 2006. JNK1 deficiency does not enhance muscle glucose metabolism in lean mice. Biochemical and Biophysical Research Communications 350:1063–1068.
[32] Lark, D.S., Torres, M.J., Lin, C.-T., Ryan, T.E., Anderson, E.J., Neufer, P.D., 2016. Direct real-time quantification of mitochondrial oxidative phosphorylation efficiency in permeabilized skeletal muscle myofibers. American Journal of Physiology - Cell Physiology 311(2):C239–C245.
[33] Tarpey, M.D., Valencia, A.P., Jackson, K.C., Amorese, A.J., Balestrieri, N.P., Renegar, R.H., et al., 2019. Induced in vivo knockdown of the Brca1 gene in skeletal muscle results in skeletal muscle weakness. Journal of Physiology 597(3):869–887. https://doi.org/10.1113/JP276863.
[34] Torres, M.J., Kew, K.A., Ryan, T.E., Pennington, E.R., Lin, C. Te., Buddo, K.A., et al., 2018. 17β-estradiol directly lowers mitochondrial membrane microviscosity and improves bioenergetic function in skeletal muscle. Cell Metabolism 27(1):167–179.
[35] Fisher-Wellman, K.H., Lin, C.-T., Ryan, T.E., Reese, L.R., Gilliam, L.A.A., Cathey, B.L., et al., 2015. Pyruvate dehydrogenase complex and nicotinamide nucleotide transhydrogenase constitute an energy-consuming redox circuit. Biochemical Journal 467(2):271–280.

[36] Spangenburg, E.E., Le Roith, D., Ward, C.W., Bodine, S.C., 2008. A functional insulin-like growth factor receptor is not necessary for load-induced skeletal muscle hypertrophy. Journal of Physiology 586(1):283–291.

[37] Tarpey, M.D., Amorese, A.J., Balestrieri, N.P., Ryan, T.E., Schmidt, C.A., McClung, J.M., et al., 2018. Characterization and utilization of the flexor digitorum brevis for assessing skeletal muscle function. Skeletal Muscle 8(1): 1–15. https://doi.org/10.1186/s13395-018-0160-3.

[38] Barros, R., Machado, U.F., Warner, M., Gustafsson, J.-A., 2006. Muscle GLUT4 regulation by estrogen receptors ERbeta and ERalpha. Proceedings of the National Academy of Sciences 103(5):1605–1608.

[39] Barros, R., Gabbi, C., Morani, A., Warner, M., Gustafsson, J.-A., 2009. Participation of ERalpha and ERbeta in glucose homeostasis in skeletal muscle and white adipose tissue. American Journal of Physiology - Endocrinology And Metabolism 297(1):E124–E133.

[40] Anderson, E.J., Lustig, M.E., Boyle, K.E., Woodlief, T.L., Kane, D.a., Lin, C., et al., 2009. Mitochondrial H2O2 emission and cellular redox state link excess fat intake to insulin resistance in both rodents and humans. Journal of Clinical Investigation 119(3):573–581.

[41] Fisher-Wellman, K.H., Neufer, P.D., 2012. Linking mitochondrial bioenergetics to insulin resistance via redox biology. Trends in Endocrinology and Metabolism 23(3):142–153.

[42] Klinge, C.M., 2017. Estrogens regulate life and death in mitochondria. Journal of Bioenergetics and Biomembranes 49(4):307–324.

[43] Jackson, K.C., Wohlers, L.M., Lovering, R.M., Schuh, R.a., Maher, A.C., Bonen, A., et al., 2013. Ectopic lipid deposition and the metabolic profile of skeletal muscle in ovariectomized mice. American Journal of Physiology - Regulatory, Integrative and Comparative Physiology 304(3):R206–R216.

[44] Camporez, J.P.G., Jornayvaz, F.R., Lee, H.Y., Kanda, S., Guigni, B.a., Kahn, M., et al., 2013. Cellular mechanism by which estradiol protects female ovariectomized mice from high-fat diet-induced hepatic and muscle insulin resistance. Endocrinology 154(3):1021–1028.

[45] Wohlers, L.M., Powers, B.L., Chin, E.R., Spangenburg, E.E., 2013. Using a novel coculture model to dissect the role of intramuscular lipid load on skeletal muscle insulin responsiveness under reduced estrogen conditions. American Journal of Physiology - Endocrinology And Metabolism 304(11):E1199–E1212.

[46] Bondesson, M., Hao, R., Lin, C.-Y., Williams, C., Gustafsson, J.-Å., 2015. Estrogen receptor signaling during vertebrate development. Biochimica et Biophysica Acta 1849(2):142–151.

[47] Kaludjerovic, J., Ward, W.E., 2012. The interplay between estrogen and fetal adrenal cortex. Journal of Nutrition and Metabolism, 1–12.

[48] Byrne, K., Vuocolo, T., Gondro, C., White, J.D., Cockett, N.E., Hadfield, T., et al., 2010. A gene network switch enhances the oxidative capacity of ovine skeletal muscle during late fetal development. BioMed Central Genomics 11(1):378.

[49] Kim, Y., Yang, D.S., Katti, P., Glancy, B., 2019. Protein composition of the muscle mitochondrial reticulum during postnatal development. The Journal of Physiology, 1–21.

[50] Luquet, S., Perez, F.A., Hnasko, T.S., Palmiter, R.D., 2005. NPY/AgRP neurons are essential for feeding in adult mice but can be ablated in neonates. Science 310(5748):683–685.

[51] Vieira Potter, V.J., Strissel, K.J., Xie, C., Chang, E., Bennett, G., Defuria, J., et al., 2012. Adipose tissue inflammation and reduced insulin sensitivity in ovariectomized mice occurs in the absence of increased adiposity. Endocrinology 153(9):4266–4277.

[52] Wu, H., Ballantyne, C.M., 2017. Skeletal muscle inflammation and insulin resistance in obesity. Journal of Clinical Investigation 127(1):43–54.

[53] Ciana, P., Di Luccio, G., Belcredito, S., Pollio, G., Vegeto, E., Tatangelo, L., et al., 2001. Engineering of a mouse for the in vivo profiling of estrogen. Molecular Endocrinology 15:1104–1113.

